

Flow Through, Immunomagnetic Cell Separation

Jeffrey J. Chalmers,^{*,†} Maciej Zborowski,^{*,‡} Liping Sun,[†] and Lee Moore[‡]

Department of Chemical Engineering, The Ohio State University, 140 West 19th Avenue, Columbus, Ohio 43210, and Department of Biomedical Engineering, The Cleveland Clinic Foundation, 9500 Euclid Avenue, Cleveland, Ohio 44195

A brief, process-oriented overview of immunologically based cell separation technology is presented. In addition, the design and preliminary experimental data of two unique flow-through immunomagnetic cell separation devices are presented. The first design is based on a dipole magnetic field, while the second design is based on a quadrupole magnetic field. The dipole design can "fractionate" an inlet, magnetically labeled, cell stream into different outlet streams on the basis of the degree to which the cell is immunomagnetically labeled. The quadrupole separator splits an inlet, immunomagnetically labeled, cell stream into two outlet streams in which the purity, recovery, and potentially the degree to which the cells are immunomagnetically labeled is controlled by the flow rates in the inlet and outlet flows. A 99% purity and 86% recovery have been achieved with this system. Some distinct advantages of these two systems are the potential of high purity, recovery, and throughput at a cost which is potentially significantly lower than current, comparable technologies.

Introduction

Overview of Immunologically Based Analytical and Separation Technologies. The ability to analyze and separate a heterogeneous cell population on the basis of cellular properties/characteristics is a significant analytical and preparative resource. During the last two decades, significant advances have been made in immunology, and various types of cellular probes have become available. These probes have resulted in the ability of researchers and clinicians to differentiate cells based upon the presence of specific surface marker(s) (in many cases specific receptors) as well as intrinsic internal characteristics. The list of properties/characteristics analyzed exceeds the objective of this paper; however, examples include DNA content, cellular pigment content, total protein content, intracellular pH, membrane organization, and probably the most important characteristic from a clinical point of view, the presence of specific surface markers (receptors) (e.g., presence of CD4 and CD8 on lymphocytes) (1).

The key to being able to conduct such analysis or separation is the ability to identify, or label, the property/characteristic of interest. In the case of separations, after labeling, one needs to exploit this label as a "handle" to remove the cell(s) from the rest of the population. A variety of labels and "handles" are used in a number of different technologies. The most specific labels are those that bind only to specific cell-associated molecules.

While a number of these highly specific labels exist, the most commonly used are antibodies (a second type of labeling interaction is streptavidin interaction which will not be discussed further (2)). Typically, these antibody labels are then covalently linked to either a

molecule, a particle, or a support matrix. These covalent linkages can be classified into three categories which reflect the properties of the compound the antibody is linked to: *immunofluorescent*, *immunomagnetic*, or *immunosolid/immunomatrix*.

The most commonly used *immunofluorescent* technology for cell separation is fluorescence-activated cell scanning/sorting (FACS). FACS systems can be used for both analysis and sorting. Applications of this technology range from basic biological and biotechnological practices to the diagnosis and treatment of human disease (3). The primary application of *immunomagnetic* labels is for cell separation; however, a simple analytical device is available (4, 5). A number of commercial, *immunomagnetic* separation technologies exist (MPC separator series, Dynal AS, Trondheim, Norway; MACS system, Miltenyi Biotec GmbH, Bergisch Gladbach, Germany; Immunicon, Huntington Valley, PA), and again, the applications run from basic biological and biotechnological applications to the treatment of human disease (6-11). Commercial applications of *immunosolid/immunomatrix* separations range from the attachment of the specific antibody to the bottom of a vessel (immunopanning) (12, 13) to the attachment of the specific antibody to packing material within a column (CEPRATE, CellPro Inc., Bothell, WA) (14-16). These applications are limited to cell separations only.

With respect to cell separation, commercial applications of each of the three categories of conjugated labels have distinct advantages and disadvantages. Commercial examples of technologies using each of these three categories of conjugated labels are compared in Table 1. The information and data presented in Table 1 come from company brochures and a paper by de Wynter et al. (17) in which the separation of CD34+ (stem cells) from human bone marrow, umbilical cord, and peripheral blood was compared using five different techniques. In addition, preliminary results from the two new separation devices discussed in this paper are included for

* Corresponding authors.

† The Ohio State University. Tel: (614) 292-2727. Fax: (614) 292-3769. E-mail: Chalmers.1@osu.edu.

‡ The Cleveland Clinic Foundation. Tel: (216) 445-9330. Fax: (216) 444-9198. E-mail: zborow@bme.ri.ccf.org.

Table 1. Summary of Different Cell Separation Technologies (Isolation of Hematopoietic Stem Cells and Human Lymphocytes)

method	mode	decision-making process	throughput (cells/s)	purity (%)	recovery (%)
FACS	flow	serial	10^3-10^4	>70	>40
Mini MACS (colloid magnetic beads)	batch	parallel	10^6	>70	60
Dynabeads, MPC (particulate, magnetic beads)	batch	parallel	10^7	>30	>5
CELLector Flasks (panning technique)	batch	parallel		33	15.1
CEPRATE, CellPro (avidin-coated beads in column)	batch	parallel	10^7	70	40
quadrupole, immunomagnetic separator	flow	parallel	10^3	99	60-86
dipole, immunomagnetic separator	flow	parallel	10^2-10^3	98	37

comparison. The mode of operation refers to whether a cell flows through, or is retained within, the device. The decision-making process refers to how a cell is evaluated with respect to whether it is "positive" or "negative" for the given cell marker. Finally, all of the systems evaluated in Table 1 separate cells (except FACS), practically speaking, in a *binary* mode of operation—either the cell has a sufficient amount of label bound to result in a separation or it does not. Strictly speaking, a FACS system can separate cells in a ternary mode of operation: positive, negative, or null. Also, multiple lasers and/or wavelengths and, correspondingly, multiple parameters can be used to identify the cell of interest. An interesting quote from the paper by de Wynter et al. (17) is "Though FACS sorting has often been the method of choice for generating pure populations of cells, if large numbers of rare cells are required, this method is not suitable." It should also be noted that FACS is the most expensive technique listed with respect to initial capital investment and dedication of personnel once the system is purchased.

Since the focus of this paper is immunomagnetic cell separation, the remainder of this paper will discuss the development of immunomagnetic cell separation technologies which combine the advantages of several of the different technologies listed in Table 1. In particular, preliminary results of two immunomagnetic, cell separation technologies will be presented which combine the advantages of a flow through mode of operation, a parallel decision-making process, a potential for high purity and recovery, and the potential of high throughput, all at a low cost (when compared to FACS). In addition, these technologies have the potential to separate cells in an *analog* mode of operation, i.e., the potential to "fractionate" a positively labeled population into subfractions on the basis of the degree to which the cell is labeled.

Fundamentals of Immunomagnetic Cell Separation. The fundamental force acting on a paramagnetic entity is given by (18)

$$\mathbf{F}_b = \frac{1}{2\mu_0} \Delta\chi V_b \nabla B^2 \quad (1)$$

where \mathbf{F}_b is the magnetic force acting on the paramagnetic entity of volume V_b , $\Delta\chi$ is the difference in magnetic susceptibility between the magnetic bead, χ_b , and the surrounding medium, χ_f , μ_0 is the magnetic permeability of free space, B is the external magnetic field, and ∇ is the gradient operator.

Immunomagnetic labels (in this case, specific antibodies linked to paramagnetic entities) can be classified into three groups on the basis of the size of the paramagnetic entity: *particulate* (on the order of a cell diameter, typically 1–5 μm), *colloidal* (on the order of 100 nm), and *molecular* (on the order of 10 nm). A number of particulate and colloidal immunomagnetic labels can be pur-

chased commercially (Dynal AG, Oslo, Norway; Miltenyi Biotec GmbH, Bergisch Gladbach, Germany; Immunicon, Huntingdon Valley, PA), while the third, molecular, is available from research labs (19). With respect to the size of the paramagnetic entity, two important points need to be made. First, the degree of paramagnetism is directly proportional to the size of the entity. Second, the size of the paramagnetic entity significantly effects the distribution of the degree to which a cell can be paramagnetically labeled.

The actual paramagnetic force acting on a labeled cell can be represented by

$$\mathbf{F}_m = A_c \alpha \beta \mathbf{F}_b \quad (2)$$

where \mathbf{F}_m is the magnetic force acting on the cell, A_c is the surface area of the cell, α is the number of specific cell surface markers per membrane surface area, β is the number of antibody magnetic bead complexes bound per receptor, and \mathbf{F}_b is the magnetic force acting on a single label particle.

In opposition to this magnetic force, a suspended cell would experience a drag force which is described by

$$\mathbf{F}_d = 3\pi \mathbf{v}_c D_c \eta \quad (3)$$

Here \mathbf{v}_c is the magnetically induced velocity (relative to the medium), D_c is the diameter of the cell, and η is the viscosity of the suspending medium.

Applying Newton's Second Law, and considering for simplicity that cell buoyancy is negligible, one obtains the following equation:

$$\mathbf{F}_m + \mathbf{F}_d = m\mathbf{a} \quad (4)$$

where m is cell mass and \mathbf{a} is its acceleration. It was demonstrated for Dynal beads, by Reddy et al. (20), that the \mathbf{F}_m and \mathbf{F}_d terms are several orders of magnitude greater than the inertial $m\mathbf{a}$ term. As discussed above, Dynal beads, which can be classified as *particulate* labels, are several orders of magnitude greater in paramagnetic susceptibility than typical colloidal or molecular labels. Consequently, it will be assumed that the right-hand side of eq 4 can be set equal to zero.

By substituting eqs 2 and 3 into eq 4, setting eq 4 equal to zero, replacing A_c by the expression for the surface area of a sphere, assuming $\beta = 1$, and solving for \mathbf{v}_c , one obtains

$$\mathbf{v}_c = \frac{D_c \alpha \mathbf{F}_b}{3\eta} \quad (5)$$

This relationship (eq 5) demonstrates that the variables D_c , α , and \mathbf{F}_b control the paramagnetically induced velocity of a labeled cell. Conversely, if one is capable of measuring \mathbf{v}_c then one may determine α , providing values for \mathbf{F}_b and D_c are available.

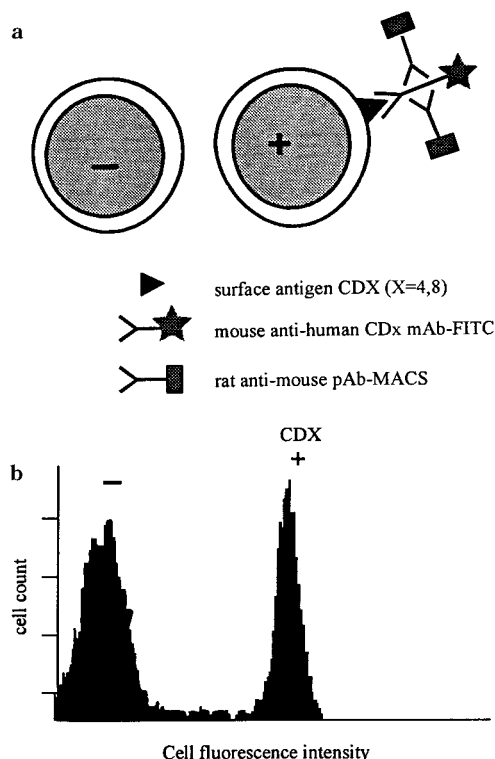


Figure 1. (a) Diagram of the immunomagnetic labeling protocol. (b) FACS histogram of CD4 immunomagnetically labeled cells.

If one were able to design a device in which this induced velocity could be well controlled and directed, it would be possible to exploit this induced velocity to direct immunomagnetically labeled cells into various fluid streams on the basis of the degree to which the cells are paramagnetically labeled. In the remainder of this paper, two devices in which this is possible will be presented.

Experimental Methods

Cells Used. Peripheral blood was obtained by venipuncture from healthy donors in accordance with the Cleveland Clinic Foundation (CCF) Institutional Review Board (IRB) regulations. The Ficoll-Paque technique was used to obtain peripheral blood mononuclear (PBMN) cells, by layering diluted blood over a Ficoll cushion (Pharmacia, Uppsala, Sweden), centrifuging, and collecting cells at the interface.

Magnetic Labeling Procedure. A previously published, two-step immunofluoromagnetic labeling procedure was used (21). The procedure allows for both magnetic separation and flow cytometry analysis. The cells were first labeled with mouse, anti-human CDx monoclonal antibody (mAb) conjugated to fluorescein isothiocyanate (FITC) (B-D Immunocytometry systems, San Jose, CA). Next, the cells were labeled with either a rat anti-mouse polyclonal antibody (pAb) conjugated to an iron dextran colloid or a rat anti-FITC pAb-iron-dextran conjugate (MACS microbeads, Miltenyi Biotec GmbH, Bergisch Gladbach, Germany). Figure 1a presents a diagram of this labeling procedure, and Figure 1b presents a FACS histogram of these labeled cells.

Separation Devices. Two prototype separation devices have been constructed. The first device, based on a dipole magnetic field, and referred to as a *dipole separator*, has the potential to fractionate a single stream of immunomagnetically labeled and unlabeled cells into

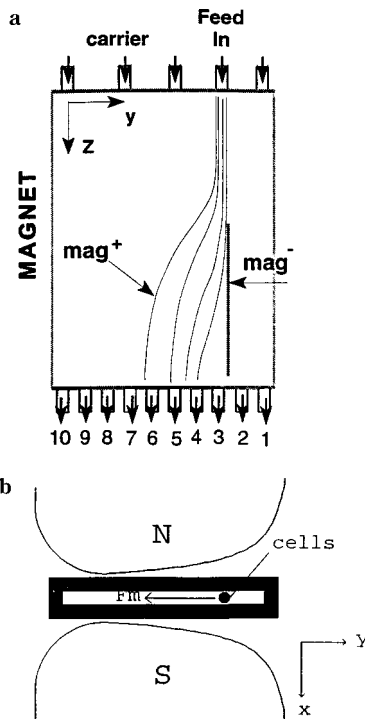


Figure 2. Schematic diagrams: (a) side view and (b) top view of the dipole separator. A constant magnetic force, directed in the $-y$ direction, is created by the unique magnet design. A cell suspension, injected in the top port indicated, flows downward with the carrier buffer injected in the other ports. Immunomagnetically labeled cells migrate in the $-y$ direction, while unlabeled cells are not deflected and continue downward in the direction indicated. Cells, deflected to various degrees, are collected in the different exit streams at the bottom of the channel. It is assumed that the deflection of the cells is proportional to the number of bound beads, and correspondingly, to the number of surface receptors/markers.

multiple exit streams. The second prototype separation device, based on a quadrupole magnetic field, is referred to as a *quadrupole separator*. Unlike the dipole separator, this design takes a single input stream of labeled and unlabeled cells and “splits” this stream into two exit streams of highly labeled and low or nonlabeled cells. This “split” is on the basis of the operating conditions which affect the distribution and residence time of the cells within the magnetic field gradient.

Dipole Separator. It is assumed that the immunomagnetic labeling protocol provides a direct proportionality between the number of surface markers on a cell and the number of bound magnetic beads. Thus, the magnetic migration velocity depends on the surface marker density and the diameter of the cell, as shown in eq 5. By making use of this feature and the constant magnetostatic energy gradient, $\frac{1}{2}\nabla B^2$ achievable with a unique pole piece geometry (Figure 2b, top view), labeled cells migrate perpendicular to the direction of flow at a rate proportional to their surface marker densities (Figure 2a). This permits separation of the injected cells into multiple outlet streams based, theoretically, on the degree to which the cells are paramagnetically labeled. This is practically achieved by injecting labeled and unlabeled cells in a single stream at the top of the channel and collecting cells in different streams at the bottom of the channel. The theoretical trajectories of paramagnetically labeled and unlabeled cells are shown in Figure 2a (side view).

The magnetic field was generated with a permanent magnet assembly consisting of four pairs of neodymium-

iron–boron magnets of $2 \times 2 \times \frac{1}{2}$ in. characterized by a maximum energy product of 2.23×10^5 (T A)/m. Soft-iron pole pieces conveyed the flux from both magnetic circuits through the interpolar air gap. The length of the interpolar gap along the z -axis was approximately 3 in. (76.2 mm). The gap between the pole pieces (interpolar gap) was maintained at 3.2 mm at its narrowest span to accommodate the glass channel.

Quantitative maps of the magnetic energy gradient $\frac{1}{2}\nabla B^2$, were obtained by a combination of experimental measurements and computer modeling. Actual magnetic field measurements were made using a gauss meter and Hall-effect probe (Model 9200 gaussmeter and transverse probe STG920404, F. W. Bell, Orlando, FL). These measurements were used to calibrate output from Magneto (Integrated Engineering Software, Winnipeg, Manitoba) field modeling software.

The flow chamber consisted of a large aspect-ratio, rectangular glass channel (1×15 mm i.d., 1.1 mm wall) (Vitro Dynamics, Inc., Rockaway, NJ). Special end caps were fabricated containing holes through which 21-gauge injectors were inserted. Lengths of $\frac{1}{32}$ in. i.d. Teflon tubing were attached to the injectors at one end and to 20-gauge blunts fitted to syringes at the other end. Two identical multisyringe pumps (Harvard Apparatus, Inc., South Natick, MA) were used in infuse/refill modes ensuring controlled flow through the system.

Quadrupole Separator. Unlike the dipole separator which achieves a constant magnetostatic energy gradient, $\frac{1}{2}\nabla B^2$, within a specific region, a quadrupole magnetic field creates a linearly increasing (in the r coordinate) magnetic energy gradient which is independent of θ and z . This results in deflection of injected, immunomagnetically labeled cells in the radial direction as they flow through the quadrupole magnetic field.

As the name implies, four magnetic “poles” focus the magnetic field around a central, cylindrical area. A side (Figure 3a) and top view (Figure 3b) of the quadrupole magnetic separator design is presented in Figure 3. The actual magnetic field is created by four pairs of permanent magnets (neodymium–iron–boron) ($2 \times 2 \times \frac{1}{2}$ in.) characterized by a maximum energy product of 2.23×10^5 (T A)/m and four steel pole pieces with a circular shape at the pole tips. The actual field created by this arrangement was measured by a gaussmeter and Hall-effect probe. The field flux density, B_0 , measured at the pole tips was 0.9 T, and a uniform magnetic gradient in the radial direction, 0.18 T/mm, was achieved.

The flow device constitutes two cylindrical flow splitters, an outer cylinder, and a coaxial solid rod. The cylinders in the separator were made of 2.38 mm i.d. and 4.41 mm i.d. brass tubing, and all of the surfaces that contacted the cells were gold plated. Cell suspensions and sheath fluid were delivered and collected from the separator through the use of syringe pumps (Harvard Apparatus, Inc., South Natick, MA).

Feed and effluent fractions collected from both the dipole and quadrupole separator were washed, fixed in 0.5% p -formaldehyde solution, and stored overnight in the refrigerator. Flow cytometry data acquisition and analysis were performed on these samples using FACS-can Analyzer and Cell Quest software (Benton-Dickinson, San Jose, CA).

Results

Dipole Separator. Results of an experiment in the dipole separator, in the form of FACS histograms of the feed and exit streams for immunomagnetically labeled

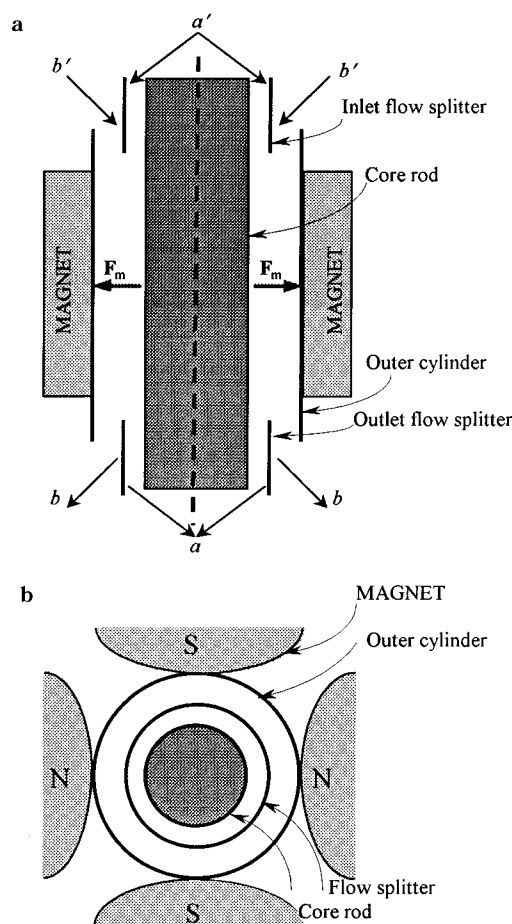


Figure 3. Schematic diagrams: (a) side view and (b) top view of the quadrupole separator. In contrast to the dipole separator, the magnetic force in the quadrupole separator increases linearly in the r direction. A cell suspension is injected in the inner, annular flow, a' , while the carrier flow is injected in the outer, annular flow, labeled b' . As the cell suspension flows down through the separator, immunomagnetically labeled cells are deflected in the r direction. If sufficiently deflected, the cells are caught in the lower, outer annular flow, b . Undeflected, or weakly deflected, cells follow the inlet streamlines and are collected in the inner annular flow, a .

CD4 lymphocytes, are presented in Figure 4a,b. Figure 4c presents percent cell recovery per exit stream. The flow cytometry histograms of the corresponding streams include the purity of the M1 gated fraction. The “M1 gated” fraction refers to a technique in FACS analysis in which a threshold fluorescence intensity (FI) is selected based on isotype control. Any cell with a FI equal or higher than this threshold is considered “positive” and is counted. In the present case, the threshold is set at 10^1 .

As the magnetic cells are deflected an increasing distance from the bulk feed stream, their purities increase, until the seventh exit stream. We believe that this decrease in purity beyond the seventh stream is a combination of very few cells magnetic enough to reach the far left stream and the clumping of unlabeled cells to the highly labeled cells which then become unclumped as they are run through the FACS (hence a few unlabeled cells greatly lowers the purity).

In addition to a histogram, a FACS analysis of cells provides statistical data including the mean fluorescence intensity of the “positive” cell fraction defined by the setting of the M1 gate. If one makes the assumption that the FI is proportional to the number of cell surface markers (receptors) (22), then the mean FI is a measure

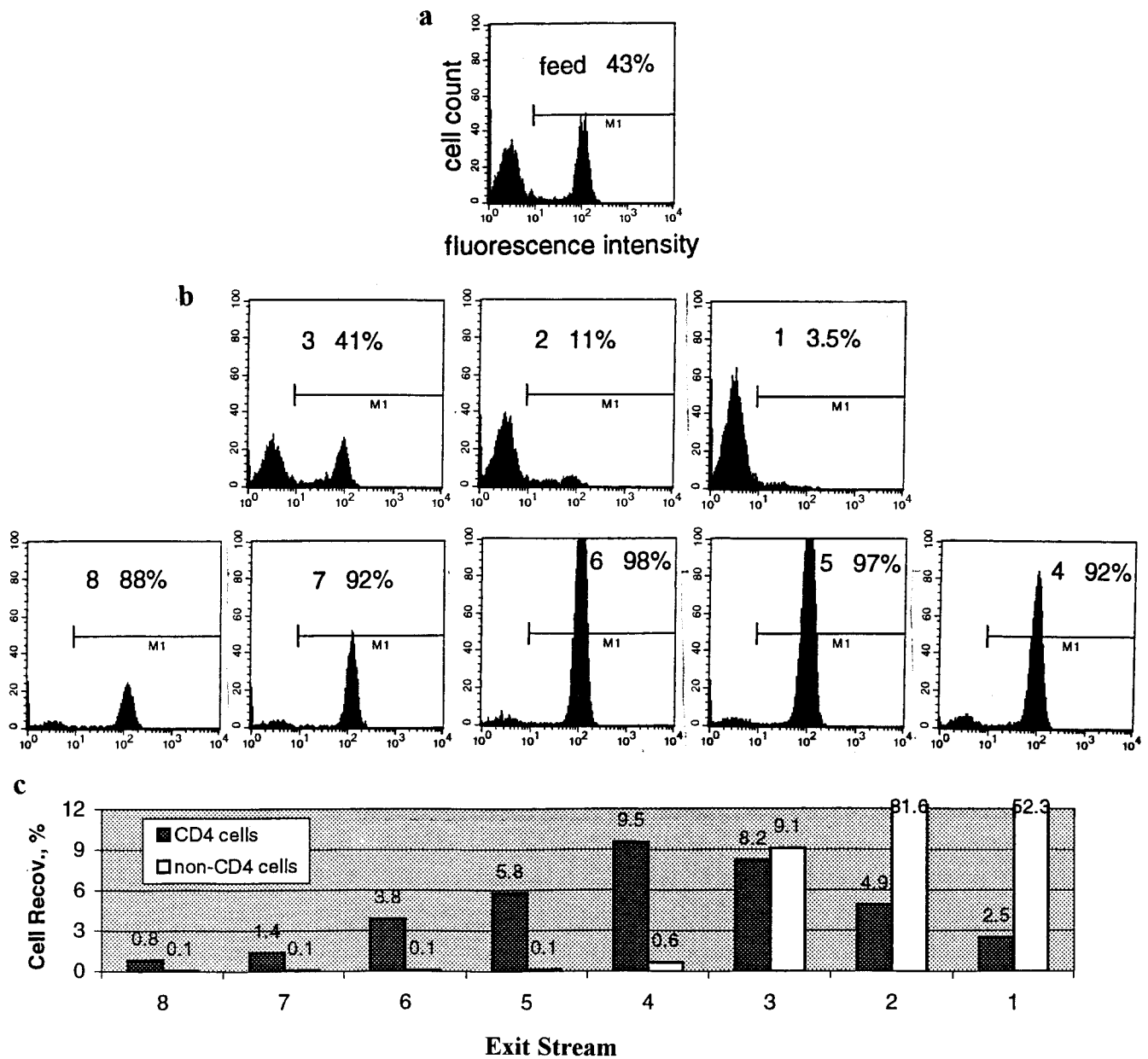


Figure 4. Representative FACS histograms of the feed cell (a) suspension and eight of the ten outlet flows (b) from the dipole separator. In this experiment, the separation of immunomagnetically and fluorescently labeled human CD4 lymphocytes was evaluated. Panel c presents the percent cell recovery as a function of the outlet flow streams.

Table 2. Results of an Experiment Using Immunomagnetically Labeled Human CD4+ Lymphocytes in the Dipole Magnet Separator

	feed stream	outlet stream							
		1	2	3	4	5	6	7	8
primary antibody									
secondary antibody									
concn (cells/mL)	4.8×10^6	2.9×10^5	4.9×10^5	2.1×10^5	9.8×10^4	6.3×10^4	4.0×10^4	1.6×10^4	9.6×10^3
flow rate (mL/min)	8.3×10^{-3}	4.6×10^{-2}	1.65×10^{-2}	1.65×10^{-2}	1.65×10^{-2}	1.65×10^{-2}	1.65×10^{-2}	1.65×10^{-2}	1.65×10^{-2}
purity, % (no. of positive cells/no. of total cells) $\times 100$	43.3	3.5	10.6	40.8	91.9	97.1	97.9	92.4	88.0
recovery, % (no. of positive cells/no. of positive cells in feed)	—	2.5	4.9	8.2	9.5	5.8	3.8	1.4	0.84
fluorescence intensity (FI) _i /(FI) _{feed}	95	21	37	72	90	98	105	116	112
throughput (cells/s)	664	222	135	58	27	17	11	4.4	2.6

of the total number of receptors on the cell. Table 2 provides a summary of the operating conditions and results of the data presented in Figure 4. Of special

interest is the mean FI as a function of entrance and exit streams. Notice the increase in FI as one moves away (to the left in Figure 2) from the entrance stream. This

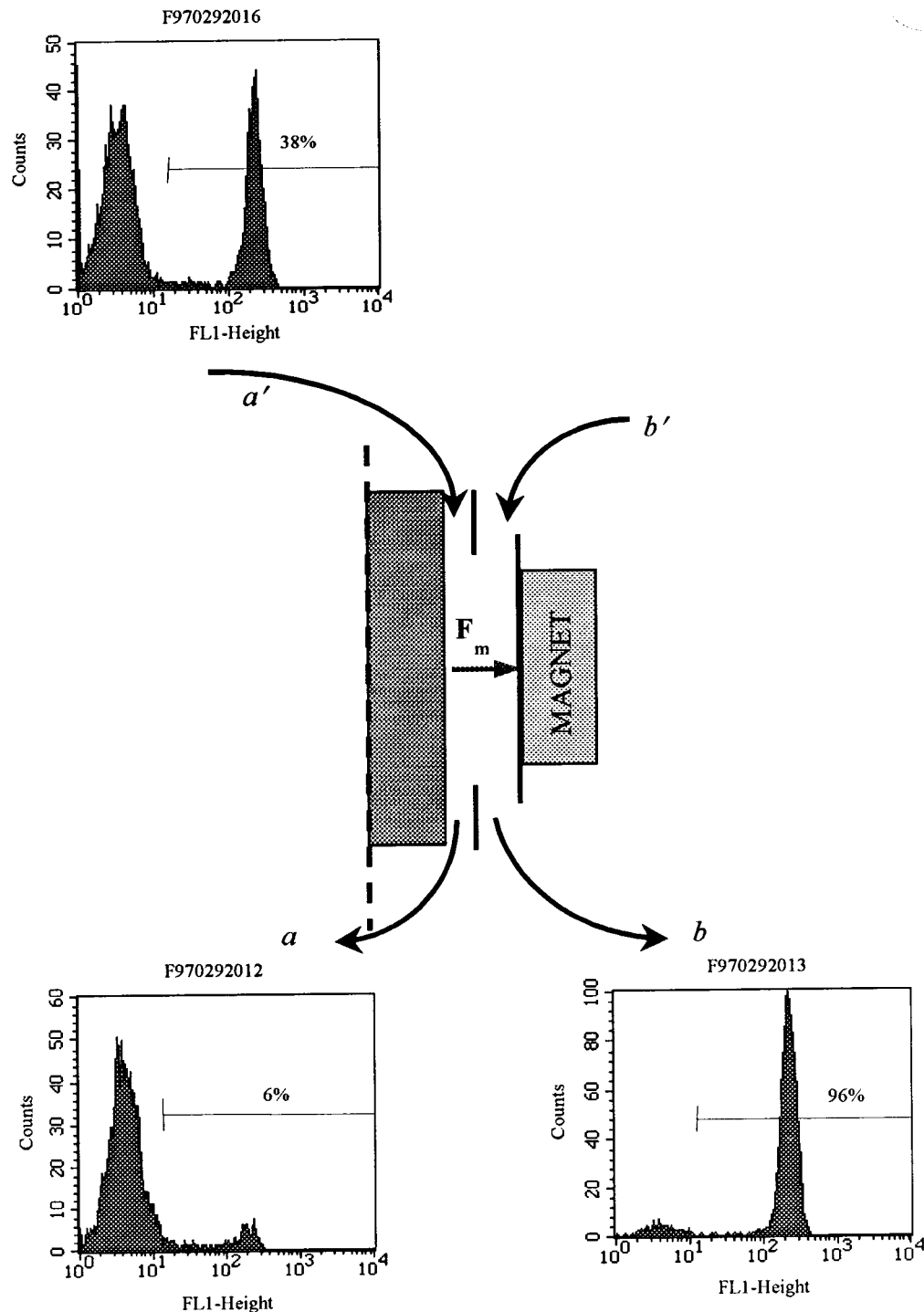


Figure 5. Representative FACS histograms of the feed cell suspension and the two outlet flows from the quadrupole separation system. In this experiment, the separation of immunomagnetically and fluorescently labeled human CD4 lymphocytes was evaluated.

is a clear indication that the entrance stream is being "fractionated" into different streams on the basis of the total number of paramagnetic particles bound to the cell surface and, presumably, the number of cell surface receptors.

Quadrupole Separator. Both enrichment and depletion were achieved with one pass through the system with paramagnetically labeled CD4 human lymphocytes, as shown in Figure 5. The upper part of Figure 5 presents a FACS histogram of a cell suspension before being introduced into the separator (fraction *a'*). As indicated, 38% of the cells are labeled as positive for CD4. To assist in the interpretation of these data, a schematic of one-half of the separator is shown in the middle part.

Lower parts present the histograms of the outlet flows. Most of the cells (96%) in the outer, outlet flow *b* are labeled CD4 lymphocytes, while in the inner, outlet flow *a*, only 6% of the cells are positively labeled. In this case, about 2000 cells were processed per second.

A second experiment, presented in Figure 6, demonstrated the potential of cell enrichment of CD8-labeled human lymphocytes. In this case, 26% of the feed was positively labeled, while the outer, outlet flow *b* was enriched to 99% CD8 cells and the inner, outlet flow *a* was depleted to 12%. In this case, about 2000 cells were processed per second. Table 3 summarizes the operating conditions and the results of these two experiments.

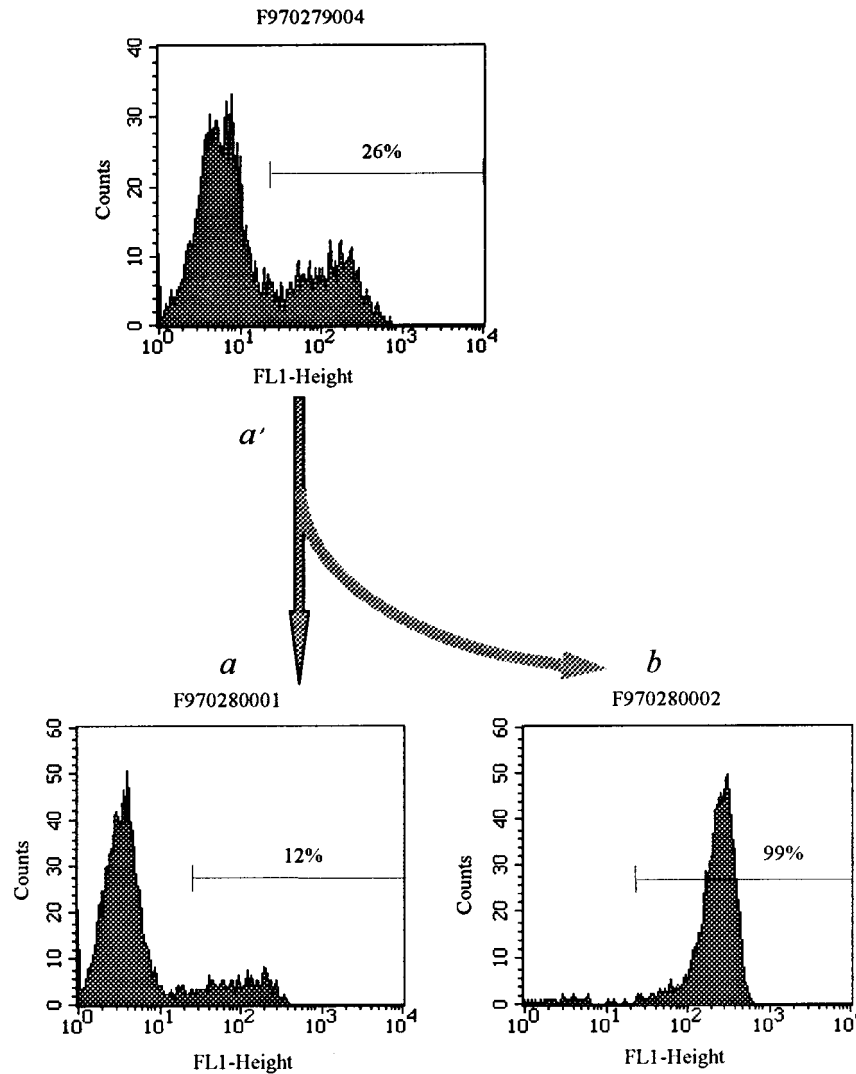


Figure 6. Representative FACS histograms of the feed cell suspension and the two outlet flows from the quadrupole separation system. In this experiment the separation of immunomagnetically and fluorescently labeled human CD8 lymphocytes was evaluated.

Table 3. Results of Two Experiments Using Immunomagnetically Labeled Human Lymphocytes in the Quadrupole Separator

	expt 1		expt 2	
primary antibody	anti CD4		anti CD8	
secondary antibody	Rat anti mouse (pAb) -MACS		Rat anti mouse (pAb) -MACS	
purity in feed (%)	38		26	
inlet	a'	b'	a'	b'
cell concn (cells/ml)	1.0×10^6		1.0×10^6	
flow rate (mL/min)	0.1	1.9	0.125	2.375
outlet	a	b	a	b
flow rate (mL/min)	0.4	1.6	0.5	2
purity (%)	6	96	12	99
recovery (%)	5.1	85.9	25.4	64.4
throughput (cells/s)	1667		2083	

Discussion

Two prototype, flow through, immunomagnetic cell separations systems have been designed and tested. In contrast to other immunomagnetic cell separators, these two designs are continuous (flow through) as opposed to the current commercial devices which are batch. While the current dipole prototype is slower (relative to the quadrupole and FACS systems), it has the potential to “fractionate” a single cell stream into multiple streams of different immunomagnetic susceptibility. The quadrupole separator, while only making a binary split in a single pass, has a higher throughput compared to the

dipole, has the potential for high purity and recovery, and has the potential of being staged or operated in recycle mode.

It should be noted that both of these designs are prototypes and have not been optimized. With respect to the dipole separator, in the run presented, only approximately 37% of the positive cells were recovered in the various exit streams. We believe that there are a number of reasons for this loss. One reason is the inability to recover all the input cell suspension because of the relatively small samples injected into the separator when compared to the larger volume of fluid contained

within the whole channel and difficulty in recovering this fluid. A second possible reason is cells becoming attached to the wall. Current work in our laboratory is addressing these and other issues such as throughput.

With respect to the quadrupole separator, only two of a large number of experiments, operated under different conditions, were presented to demonstrate the capability of high recovery or high purity. The difference in the performance of the separator, i.e., purity and recovery, we believe is the result of the different operating conditions and the degree to which the cells are immunomagnetic (there are three times as many CD8 markers on a lymphocyte when compared to CD4 markers). Ongoing research is developing the theoretical basis for these observations.

Recently, Chalmers et al. (23) developed the mathematical relationships which defined the theoretical limits for the number of fractions into which immunomagnetically labeled cell populations can be separated upon the basis of a range in cell surface marker density and distribution in cell size. Also, a significant analogy can be drawn between the hydrodynamic behavior in the cylindrical columns in the quadrupole separator and split-flow thin channel separations (SPLIT) (24). These relationships and others are being used to evaluate and develop second-generation separators. In addition, theoretical calculations indicate that at least 2 orders of magnitude increase in cell throughput in the quadrupole separator can be achieved. This improved throughput, combined with the low cost of fabricating the quadrupole separator (~\$5000–10,000), suggests the potential of this separation technology.

Acknowledgment

The authors thank the National Institutes of Health (CA 62349), the Whitaker Foundation (20010308), and the National Science Foundation (BCS 9258004) for their financial support.

References and Notes

- (1) Shapiro, H. *Practical Flow Cytometry*; Wiley-Lis: New York, 1995; pp 1–2.
- (2) DePalma, A. Developments in Biomagnetic Separations Focus on New Affinity Mechanisms. *Genet. Eng. News* **1997**, *17*, 11.
- (3) Shapiro, H. *Practical Flow Cytometry*; Wiley-Lis: New York, 1995; pp 1–2.
- (4) Winto-Morbach, S.; Tchikov, V.; Muller-Ruchholtz, W. Magnetophoresis: I. Detection of Magnetically Labeled Cells. *J. Clin. Lab. Anal.* **1994**, *8*, 400–406.
- (5) Zborowski, M.; Fuh, C. B.; Green, R.; Sun, L.; Chalmers, J. J. Thin-film magnetapheresis of ferritin-labeled lymphocytes. *Anal. Chem.* **1995**, *67*, 3702–3712.
- (6) Busch, J.; Huber, P.; Pfluger, E.; Miltenyi, S.; Holtz, J.; Radbruch, A. Enrichment of fetal cells from maternal blood by high gradient magnetic cell sorting (double MACS) for PCR-based genetic analysis. *Prenatal Diagn.* **1994**, *14*, 1129–1140.
- (7) Gee, A. P.; Mansour, V.; Weiler, M. T-cell depletion of human bone marrow. *J. Immunogenet.* **1989**, *16*, 103–115.
- (8) Miltenyi, S.; Muller, W.; Weichel, W.; Radbruch, A. High gradient magnetic cell separation. *Cytometry* **1990**, *11*, 231–238.
- (9) Radbruch, A.; Mechtold, B.; Thiel, A.; Miltenyi, S.; Pfluger, E. High-gradient magnetic sorting. *Methods Cell Biol.* **1994**, *42*, 387–403.
- (10) Schmitz, B.; Radbruch, A.; Kummel, T.; Wickenhauser, C.; Korb, H.; Hansmann, M. L.; Thiele, J.; Fischer, R. Magnetic activated cell sorting (MACS)—a new immunomagnetic method for megakaryocytic cell isolation: comparison of different separation techniques. *Eur. J. Hematol.* **1994**, *52*, 267–275.
- (11) Manyonda, I. T.; Soltys, A. J.; Hay, F. C. A critical evaluation of the magnetic cell sorter and its use in the positive and negative selection of CD45RO+ cells. *J. Immunol. Methods* **1992**, *149*, 1–10.
- (12) Gard, A. L.; Maughon, R. H.; Schachner, M. In vitro oligodendroglial properties of cell adhesion molecules in the immunoglobulin superfamily: Myelin-associated glycoprotein and N-CAM. *J. Neurosci. Res.* **1996**, *46*, 415–426.
- (13) Madison, D. L.; Kruger, W. H.; Kim, T.; Pfeiffer, S. E. Differential expression of rab3 isoforms in oligodendrocytes and astrocytes. *J. Neurosci. Res.* **1996**, *45*, 258–268.
- (14) Bertolini, F.; Thomas, T.; Battaglia, M.; Gibelli, N.; Pedrazzoli, P.; Robustelli Della Cuna, G. A new 'two step' procedure for 4.5 log depletion of T and B cells in allogeneic transplantation and of neoplastic cells in autologous transplantation. *Bone Marrow Transplant.* **1997**, *19*, 615–619.
- (15) Collins, P.; Watts, M.; Brocklesby, M.; Gerritsen, B.; Veys, P. Successful engraftment of haploidentical stem cell transplant for familial haemophagocytic lymphohistiocytosis using both bone marrow and peripheral blood stem cells. *Br. J. Haematol.* **1997**, *96*, 644–646.
- (16) Vogel, W.; Behringer, D.; Scheding, S.; Kanz, L.; Brugger, W. Ex vivo expansion of CD34+ peripheral blood progenitor cells: Implications for the expansion of contaminating epithelial tumor cells. *Blood* **1996**, *88*, 2707–2713.
- (17) de Wynter, E. W.; Coutinho, L. H.; Pei, X.; Marsh, J. C. W.; Hows, J.; Luft, T.; Testa, N. G., Comparison of Purity and Enrichment of CD34+ Cells from Bone Marrow, Umbilical Cord and Peripheral Blood (Primed for Apheresis) Using Five Separation Systems. *Stem Cells* **1995**, *13*, 524–532.
- (18) Zborowski, M. Physics of magnetic cell sorting. In *Scientific and Clinical Applications of Magnetic Microcarriers: An Overview*, Hafeli, U., Schutt, W., Teller, J., Zborowski, M., Eds.; Plenum: New York, 1997; pp 205–232.
- (19) Zborowski, M.; Fuh, C. B.; Green, R.; Baldwin, N. J.; Reddy, S.; Douglas, T.; Mann, S.; Chalmers, J. J. Immunomagnetic isolation of magnetoferritin-labeled cells in a modified ferromagnet. *Cytometry* **1996**, *24*, 251–259.
- (20) Reddy, S.; Moore, L. R.; Sun, L.; Zborowski, M.; Chalmers, J. J. Determination of the Magnetic Susceptibility of Labeled Particles by Video Imaging. *Chem. Eng. Sci.* **1996**, *51*, 947–956.
- (21) Zborowski, M.; Moore, L.; Sun, Liping, S.; Chalmers, J. J. Continuous-flow magnetic cell sorting using soluble immunomagnetic labels. In *Scientific and Clinical Applications of Magnetic Microcarriers: An Overview*, Hafeli, U., Schutt, W., Teller, J., Zborowski, M., Eds.; Plenum: New York, 1997; pp 247–260.
- (22) Bikoue, A.; George, F.; Poncelet, P.; Mutin, M.; Janossy, G.; Sampol, J. Quantitative Analysis of Leukocyte Membrane Antigen Expression: Normal Adult Values. *Cytometry* **1996**, *26*, 137–147.
- (23) Chalmers, J. J.; Mandal, S.; Fang, B.; Sun, L.; Zborowski, M. Theoretical Analysis of Cell Separation Based on Cell Surface Marker Density. *Biotechnol. Bioeng.*, in press
- (24) Zborowski, M.; Williams, P. S.; Sun, L.; Moore, L. R.; Chalmers, J. J. Cylindrical split and quadrupole magnetic field in applications to continuous-flow magnetic cell sorting. *J. Liq. Chromatog. Rel. Tech.* **1997**, *20*, 2887–2905.

Accepted December 10, 1997.

BP970140L